NIH Public Access
Author Manuscript
Dalton Trans. Author manuscript; available in PMC 2013 March 14.

Published in final edited form as:
Dalton Trans. 2012 March 14; 41(10): 3046–3052. doi:10.1039/c2dt11811d.

Coordination-Driven Self-Assembly of Ruthenium-Based Molecular-Rectangles: Synthesis, Characterization, Photophysical and Anticancer Potency Studies†

Vaishali Vajpayee[†], **Young Ho Song**[†], **Young Jun Jung**[‡], **Se Chan Kang**[‡], **Hyunuk Kim**[±], **In Su Kim**[†], **Ming Wang**[ζ], **Timothy R. Cook**[ζ], **Peter J. Stang**[ζ], and **Ki-Whan Chi**[†]

Se Chan Kang: sckang@semyung.ac.kr; Peter J. Stang: stang@chem.utah.edu; Ki-Whan Chi: kwchi@ulsan.ac.kr

[a]Department of Chemistry, University of Ulsan, Ulsan 680-749, Republic of Korea.

[b]Department of Natural Medicine Resources, University of Semyung, Jecheon 390-711, Republic of Korea.

[c]Department of Chemistry, POSTECH, Pohang 690-784, Republic of Korea.

[d]Department of Chemistry, University of Utah, Salt Lake City, Utah 84112-0850, U.S.A.

Abstract

A suite of eight cationic, tetra-metallic molecular rectangles (**1**–**8**) was generated via coordination-driven self-assembly using four dicarboxylate-bridged arene-Ru precursors (**A1**–**A4**) with one of two dipyridyl ligands (**D1**, **D2**). The high-yielding (84–92%) rectangles were characterized by ^{1}H NMR and HR-ESI-MS to support their structural assignments. The molecular structure of **5** was determined by single crystal X-ray analysis, which indicated that two **D2** ligands bridge two **A1** acceptors to form a rectangular construct. The photophysical properties of these metalla-rectangles and their molecular precursors were also investigated, as well as an MTT assay to evaluate the *in vitro* cytotoxicities relative to two chemotherapeutic agents, cisplatin and doxorubicin. MTT assays were conducted using SK-hep-1 (liver cancer) and HCT-15 (colon cancer) human cancer cell lines. Compounds **3**, **4**, **7** and **8** showed significant activity, with IC_{50} values comparable to those of cisplatin and doxorubicin.

Introduction

Over the past two decades, a wide variety of two-dimensional (2D) architectures have been rationally designed via metal-mediated coordination chemistry.[1] As the library of known metal-based acceptors and ligand donors expanded, judicious combinations of specifically-angled subunits led to the efficient construction of a myriad of symmetric, two-component frameworks via coordination-driven self-assembly.[2–4] This early structural work quickly evolved to address practical applications, including host-guest chemistry, sensing, catalysis and molecular flasks for organic transformations.[5–6] Pd(II) and Pt(II) ions have assumed an archetypal role as the metal acceptors in these designs, due to their tendency to form stable square planar complexes with control over the *cis* or *trans* disposition of ligands.[7, 8] However, as the principals governing coordination-driven self-assembly have been

†Electronic Supplementary Information (ESI) available: [NMR and HR-ESI-MS data for **1–8**, CCDC 841900]. See DOI: 10.1039/b000000x/

© The Royal Society of Chemistry [year]

Correspondence to: Se Chan Kang, sckang@semyung.ac.kr; Peter J. Stang, stang@chem.utah.edu; Ki-Whan Chi, kwchi@ulsan.ac.kr.

NIH-PA Author Manuscript
NIH-PA Author Manuscript
NIH-PA Author Manuscript

NIH-PA Author Manuscript

NIH-PA Author Manuscript

NIH-PA Author Manuscript

developed, the versatility afforded by alternative metal ions has become apparent, unlocking new properties and applications.[9]

Recently, organometallic half-sandwich complexes of iridium, rhodium and ruthenium have begun attracting attention as building blocks for coordination-driven self-assembly.[10] These complexes are particularly well-suited for use as "molecular clips," wherein two arene-ruthenium sites are bridged by a *bis*-bidentate ligand. The remaining substitutionally-labile sites on each metal is allowing the construction of 2D and 3D frameworks.[11] The biological activity of Ru-containing compounds has motivated the study of arene-Ru supramolecules with a focus on their anti-cancer properties.[12] As such, a growing number of Ru cages have been self-assembled which show promising results as antitumor agents in human cancer cell lines.[13]

Herein, we extend the library of potential metallo-pharmaceuticals with a suite of eight new arene-Ru rectangles. This series of [2 + 2] assembles includes four distinct oxalate-type bridging ligands between the Ru ions of the acceptors and two distinct rigid organic donors which differ in size through the use of ethynyl spacers. This builds upon recent observations that the size and type of the arene-Ru acceptors and organic linkers can influence the antitumor behaviour of the resulting self-assemblies.[14]

Rectangles **1**–**8** self-assembled over the course of 10 hours in 1:1 CH_3NO_2/CH_3OH solutions containing of equimolar amounts of **A1**–**A4** with **D1** or **D2** (Scheme 1), generating [*p*-cymene$_4$Ru$_4$(μ-C_2O_4)$_2$(μ-**D**)$_2$](OTf)$_4$ (**1**, **5**), [*p*-cymene$_4$Ru$_4$(μ-$C_6H_2O_4$)$_2$(μ-**D**)$_2$](OTf)$_4$ (**2**, **6**), [*p*-cymene$_4$Ru$_4$(μ-$C_{10}H_4O_4$)$_2$(μ-**D**)$_2$](OTf)$_4$ (**3**, **7**), [*p*-cymene$_4$Ru$_4$(μ-$C_{18}H_4O_4$)$_2$(μ-**D**)$_2$](OTf)$_4$ (**4**, **8**), [for **1**– **4**, **D** = $\mathbf{D_1}$ =1,2-di(pyridine-3-yl)ethyne, for **5**–**8**, **D** = $\mathbf{D_2}$ = 1,4-di(pyridine-3-yl)buta-1,3-diyne]. All metalla-rectangles were well-characterized by ^{1}H, ^{13}C NMR and high resolution electrospray mass spectrometry (HR-ESI-MS). A single crystal of complex **5** was used to determine its solid-state structure via X-ray crystallography. UV-Vis absorption and fluorescence spectra were also obtained. Furthermore, the *in vitro* anticancer efficacies of rectangles **1**–**8** against two different cancer cell lines were determined.

Experimental Section

General Details

The chloride analogues of arene-ruthenium acceptors **A1-A4,** [11(a), 12(b), 13(c),] their triflate derivatives[11(a)] and donors **D1**, **D2** were prepared according to literature methods. [15] Deuterated solvents were purchased from Cambridge Isotope Laboratory (Andover, MA, USA). NMR spectra were recorded on a Bruker 300 MHz spectrometer. ^{1}H NMR chemical shifts are reported relative to residual solvent signals. HR-ESI-Mass spectra of the molecular rectangles were recorded on a Micromass Quattro II triple-quadrupole mass-spectrometer using electrospray ionization and analyzed with the MassLynx software suite system. UV-Vis spectra were recorded on a Cary 100 Conc. Fluorescence titration studies were carried out on a HORIBA FluoroMax-4 fluorometer.

X-ray Structure Determination

The diffraction data from a single crystal of **5** mounted on a loop were collected at 100 K on an ADSC Quantum 210 CCD diffractometer with synchrotron radiation (λ= 0.90000 Å) at the Macromolecular Crystallography Beamline 6B1, Pohang Accelerator Laboratory (PAL), Pohang, Korea. The raw data were processed and scaled using the HKL2000 program. The structure was solved by direct methods, and refinements were carried out with full-matrix least-squares on F^2 with appropriate software implemented in the SHELXTL package. All non-hydrogen atoms were refined anisotropically, and hydrogen atoms were added to their geometrically ideal positions. CCDC-841900 contains the supplementary crystallographic

NIH-PA Author Manuscript

NIH-PA Author Manuscript

NIH-PA Author Manuscript

data for this paper. The data can be obtained free of charge at www.ccdc.cam.ac.uk/conts/retrieving.html or from the Cambridge Crystallographic Data Centre, 12, Union Road, Cambridge CB2 1EZ, UK.

Cancer Cell Growth Inhibition Assay (MTT assay)

Cells were routinely grown in Dulbecco's Modified Eagle Medium (DMEM) supplemented with 10% heat inactivated fetal bovine serum (FBS) 1% penicillin streptomycin at 37 °C and 5% CO_2. For the evolution of growth inhibition tests, cell suspensions were seeded into 96-well plates at a concentration of 5×10^4 cells per well (90 μL per well and 10 μL sample). MTT was prepared as a stock solution of 5 mg/ml in phosphate buffered saline (PBS, pH 7.2) and was filtered. Ten microliters of MTT solution was added to each well. After incubation for 4 hrs at 37 °C and 5% CO_2, 100 μL of DMSO (dimethylsulfoxide) was added to each well. The 96-well plates were read by an enzyme-linked immunosorbent assay (ELISA) reader at 570 nm for absorbance density values to determine the cell viability, the percentage of surviving cells was calculated from the ratio of absorbance of treated to untreated cells. The half-maximal inhibitory concentration (IC_{50}) values for cell growth were determined by fitting the plot of the logarithmic percentage of surviving cells against the logarithm of the drug concentration using a linear regression function.

General procedure for the synthesis of molecular-rectangles (1–8)

A solution of nitromethane-methanol (1:1, 2 mL) was added to a 1:1 molar ratio mixture of the corresponding arene-Ru acceptors (**A1**–**A4**) and 3-dipyridyl donors (**D1**–**D2)** and the resulting solution was stirred at room temperature for 10 hrs. The solution was then concentrated and diethyl ether was added to precipitate metalla-rectangles **1**–**8** as analytically pure solids.

Molecular-rectangle 1—Acceptor clip **A1** (8.6 mg, 0.01 mmol) and dipyridyl donor **D1** (1.8 mg, 0.01 mmol) were stirred in nitromethane-methanol (2 mL) for 10 hours to obtain **1** upon precipitation with diethyl ether. Isolated yield and color: 85%, yellow solid. Anal. Calcd for $C_{72}H_{72}F_{12}N_4O_{20}Ru_4S_4$: C, 41.70; H, 3.50; N, 2.70. Found: C, 41.31; H, 3.83; N, 2.94. ^{1}H NMR [300 MHz, $(CD_3)_2CO$]: δ (ppm) 8.48 (s, 4H, H_4), 8.22 (d, *J*= 6.0 Hz, 4H, H_1), 8.00 (d, *J*= 7.8 Hz, 4H, H_3), 7.51 (m, 4H, H_2), 6.18 (m, , 8H, Hcym), 6.06(m, 8H, Hcym), 3.01 (sept, 4H, $CH(CH_3)_2$), 2.33 (s, 12H, CH_3), 1.44 (dd, *J* = 6.9Hz, *J* = 6.9Hz, 24H,$CH(CH_3)_2$); ^{13}C NMR [75 MHz, $(CD_3)_2CO$]: δ (ppm) 172.0, 171.7, 156.4, 152.6, 143.3, 127.4, 122.3, 103.4, 98.7, 89.9, 83.6, 83.3, 82.9, 81.9, 31.9, 22.7, 22.5 18.1; MS (ESI) for **1** ($C_{72}H_{72}F_{12}N_4O_{20}Ru_4S_4$): 887.9 $[M - 2OTf]^{2+}$, 542.4 $[M - 3OTf]^{3+}$.

Molecular-rectangle 2—Acceptor clip **A2** (9.1 mg, 0.01 mmol) and dipyridyl donor **D1** (1.8 mg, 0.01 mmol) were stirred in nitromethane-methanol (2 mL) to obtain **2** upon precipitation with diethyl ether. Isolated yield and color: 88%, wine red solid. Anal. Calcd for $C_{80}H_{76}F_{12}N_4O_{20}Ru_4S_4.(C_2H_5)_2O$: C, 44.88; H, 3.86; N, 2.49. Found: C, 45.12; H, 3.78; N, 2.81.^{1}H NMR [300 MHz, $(CD_3)_2CO$]: δ (ppm) 8.80 (s, 4H, H_4), 8.19 (d, *J*= 6.0 Hz, 8H, $H_{1,3}$), 7.60 (m, 4H, H_2), 6.24 (br, 8H, Hcym), 6.08(br, 8H, Hcym), 5.78 (s, 4H, Hbq), 3.0 (sept, 4H, $CH(CH_3)_2$), 2.22 (s, 12H, CH_3), 1.35 (d, *J* = 6.9Hz, 24H,$CH(CH_3)_2$); ^{13}C NMR [75 MHz, $(CD_3)_2CO$]: δ (ppm) 184.0, 155.4, 142.2, 126.0, 123.4, 121.4, 119.2, 104.0, 101.6, 88.7, 83.7, 31.1, 21.5, 17.1; MS (ESI) for **2** ($C_{80}H_{76}F_{12}N_4O_{20}Ru_4S_4$): 937.9 $[M - 2OTf]^{2+}$, 575.8 $[M - 3OTf]^{3+}$.

Molecular-rectangle 3—Acceptor clip **A3** (9.6 mg, 0.01 mmol) and dipyridyl donor **D1** (1.8 mg, 0.01 mmol) were stirred in nitromethane-methanol (2 mL) to obtain **3** upon precipitation with diethyl ether. Isolated yield and color: 87%, sea-green solid. Anal. Calcd for $C_{88}H_{80}F_{12}N_4O_{20}Ru_4S_4$: C, 46.48; H, 3.55; N, 2.46. Found: C, 46.19; H, 3.70; N,

NIH-PA Author Manuscript

NIH-PA Author Manuscript

NIH-PA Author Manuscript

2.41. ^{1}H NMR [300 MHz, $(CD_3)_2CO$]: δ (ppm) 8.85 (s, 4H, H_4), 8.56 (d, *J*= 6.0 Hz, 4H, H_1), 8.07 (d, *J*= 7.8 Hz, 4H, H_3), 7.53 (m, 4H, H_2), 7.32 (s, 8H, Hnq), 6.05 (d, *J*= 6.3 Hz, 8H, Hcym), 5.85(d, *J* = 6.3 Hz, 8H, Hcym), 2.94 (sept, 4H, $CH(CH_3)_2$), 2.14 (s, 12H, CH_3), 1.34 (d, *J* = 6.9Hz, 24H,$CH(CH_3)_2$); ^{13}C NMR [75 MHz, $(CD_3)_2CO$]: δ (ppm) 171.8, 155.4, 152.6, 143.1, 138.4, 126.7, 122.2, 112.2, 104.1, 101.5, 89.7, 85.9, 83.2, 31.5, 22.5, 17.4; MS (ESI) for **3** ($C_{88}H_{80}F_{12}N_4O_{20}Ru_4S_4$): 2125.1 $[M - OTf]^+$.

Molecular-rectangle 4—Acceptor clip **A4** (10.5 mg, 0.01 mmol) and dipyridyl donor **D1** (1.8 mg, 0.01 mmol) were stirred in nitromethane-methanol (2 mL) to obtain **4** upon precipitation with diethyl ether. Isolated yield and color: 92%, green solid. Anal. Calcd for $C_{104}H_{88}F_{12}N_4O_{20}Ru_4S_4$: C, 50.48; H, 3.58; N, 2.26. Found: C, 50.52; H, 3.45; N, 2.31. ^{1}H NMR [300 MHz, $(CD_3)_2CO$]: δ (ppm) 9.01 (s, 4H, H_4), 8.87 (m, 8H, Hnd), 8.63 (d, *J*= 6.0 Hz, 4H, H_1), 7.93 (m, 12H, Hnd, H_3), 7.36 (m, 4H, H_2), 6.25 (d, *J*= 6.3 Hz, 8H, Hcym), 6.01 (d, *J* = 6.3 Hz, 8H, Hcym), 3.08 (sept, 4H, $CH(CH_3)_2$), 2.18 (s, 12H, CH_3), 1.32 (d, *J* = 6.9Hz, 24H,$CH(CH_3)_2$); ^{13}C NMR [75 MHz, $(CD_3)_2CO$]: δ (ppm) 170.1, 155.6, 152.3, 143.2, 134.7, 134.1, 128.5, 126.5, 122.1, 107.8, 103.9, 101.9, 89.6, 86.0, 82.5, 31.7, 22.7, 17.9; MS (ESI) for **4** ($C_{104}H_{88}F_{12}N_4O_{20}Ru_4S_4$): 2326.1 $[M - OTf]^{1+}$.

Molecular-rectangle 5—Acceptor clip **A1** (8.6 mg, 0.01 mmol) and dipyridyl donor **D2** (2.0 mg, 0.01 mmol) were stirred in nitromethane-methanol (2 mL) to obtain **5** upon precipitation with diethyl ether. Isolated yield and colour: 84%, brown-yellow solid. Anal. Calcd for $C_{76}H_{72}F_{12}N_4O_{20}Ru_4S_4.2H_2O$: C, 42.30; H, 3.55; N, 2.60. Found: C, 41.88; H, 3.45; N, 2.39. ^{1}H NMR [300 MHz, $(CD_3)_2CO$]: δ (ppm) 8.38 (m, 4H, H_4), 8.17 (m, 4H, H_1), 8.12 (m, 4H, H_3), 7.52 (m, 4H, H_2), 6.13 (m, 8H, Hcym), 5.99 (d, *J* = 6.0 Hz, 8H, Hcym), 2.96 (sept, 4H, $CH(CH_3)_2$), 2.31 (s, 12H, CH_3), 1.38 (d, *J* = 6.0 Hz, 24H,$CH(CH_3)_2$); ^{13}C NMR [75 MHz, $(CD_3)_2CO$]: δ (ppm) 170.9, 155.1, 152.7, 143.3, 126.6, 120.4, 102.6, 82.1, 78.0, 31.0, 21.5, 17.1; MS (ESI) for **5** ($C_{76}H_{72}F_{12}N_4O_{20}Ru_4S_4$): 911.9 $[M - 2OTf]^{2+}$, 558.4 $[M - 3OTf]^{3+}$.

Molecular-rectangle 6—Acceptor clip **A2** (9.1 mg, 0.01 mmol) and dipyridyl donor **D2** (2.0 mg, 0.01 mmol) were stirred in nitromethane-methanol (2 mL) to obtain **6** upon precipitation with diethyl ether. Isolated yield and color: 89%, wine red solid. Anal. Calcd for $C_{84}H_{76}F_{12}N_4O_{20}Ru_4S_4$: C, 45.40; H, 3.45; N, 2.52. Found: C, 45.13; H, 3.68; N, 2.71. ^{1}H NMR [300 MHz, $(CD_3)_2CO$]: δ (ppm) 8.58 (s, 4H, H_4), 8.32 (m, 4H, H_1), 8.26 (m, 4H, H_3), 7.63 (m, 4H, H_2), 6.27 (d, *J* = 6.0 Hz, 8H, Hcym), 6.07 (d, *J* = 6.3 Hz, 8H, Hcym), 5.78 (s, 4H, Hbq), 3.04 (sept, 4H, $CH(CH_3)_2$), 2.30 (s, 12H, CH_3), 1.40 (d, *J* = 6.9 Hz, 24H,$CH(CH_3)_2$); ^{13}C NMR [75 MHz, $(CD_3)_2CO$]: δ (ppm) 184.7, 157.0, 154.3, 143.7, 127.4, 121.2, 104.9, 102.7, 100.1, 84.6, 83.0, 78.6, 78.4, 32.2, 22.6, 18.3; MS (ESI) for **6** ($C_{84}H_{76}F_{12}N_4O_{20}Ru_4S_4$): 2072.4 $[M - OTf]^+$, 592.0 $[M - 3OTf]^{3+}$.

Molecular-rectangle 7—Acceptor clip **A3** (9.6 mg, 0.01 mmol) and dipyridyl donor **D2** (2.0 mg, 0.01 mmol) were stirred in nitromethane-methanol (2 mL) to obtain **7** upon precipitation with diethyl ether. Isolated yield and colour: 90%, sea-green solid. Anal. Calcd for $C_{92}H_{80}F_{12}N_4O_{20}Ru_4S_4.2H_2O$: C, 46.86; H, 3.59; N, 2.38. Found: C, 46.63; H, 3.72; N, 2.04. ^{1}H NMR [300 MHz, $(CD_3)_2CO$]: δ (ppm) 8.72 (s, 4H, H_4), 8.63 (m, 4H, H_1), 8.12 (m, 4H, H_3), 7.59 (m, 4H, H_2), 7.25 (s, 4H, Hnq), 6.04 (d, *J* = 6.3 Hz, 8H, Hcym), 5.86 (d, *J* = 6.3 Hz, 8H, Hcym), 3.00 (sept, 4H, $CH(CH_3)_2$), 2.24 (s, 12H, CH_3), 1.40 (d, *J* = 6.9 Hz, 24H,$CH(CH_3)_2$); ^{13}C NMR [75 MHz, $(CD_3)_2CO$]: δ (ppm) 172.0, 155.9, 153.7, 143.6, 138.6, 127.0, 121.0, 112.4, 104.7, 100.7, 85.1, 84.1, 78.7, 77.9, 31.6, 22.5, 17.4; MS (ESI) for **7** ($C_{92}H_{80}F_{12}N_4O_{20}Ru_4S_4$): 625.1 $[M - 3OTf]^{3+}$.

NIH-PA Author Manuscript

NIH-PA Author Manuscript

NIH-PA Author Manuscript

Molecular-rectangle 8—Acceptor clip **A4** (10.5 mg, 0.01 mmol) and dipyridyl donor **D2** (2.0 mg, 0.01 mmol) were stirred in nitromethane-methanol (2 mL) to obtain **8** upon precipitation with diethyl ether. Isolated yield and colour: 90%, green solid. Anal. Calcd for $C_{108}H_{88}F_{12}N_4O_{20}Ru_4S_4$: C, 51.43; H, 3.52; N, 2.22. Found: C, 51.73; H, 3.81; N, 2.39. ^{1}H NMR [300 MHz, $(CD_3)_2CO$]: δ (ppm) 8.90 (m, 8H, Hnd), 8.70 (m, 8H, H_1, H_4), 8.10 (m, 8H, Hnd), 7.75 (m, 4H, H_3), 7.33 (m, 4H, H_2), 6.25 (d, J = 6.3 Hz, 8H, Hcym), 6.02 (d, J = 6.0 Hz, 8H, Hcym), 3.14 (sept, 4H, $CH(CH_3)_2$), 2.25 (s, 12H, CH_3), 1.39 (d, J = 6.9 Hz, 24H,$CH(CH_3)_2$); ^{13}C NMR [75 MHz, $(CD_3)_2CO$]: δ (ppm) 170.1, 155.4, 153.2, 143.2, 134.7, 134.1, 128.3, 126.8, 120.6, 107.8, 104.6, 100.9, 85.1, 83.3, 78.2, 31.5, 22.6, 17.8; MS (ESI) for **8** ($C_{108}H_{88}F_{12}N_4O_{20}Ru_4S_4$): 1111.8 $[M - 2OTf]^{2+}$, 692.0 $[M - 3OTf]^{3+}$.

Results and Discussion

Synthesis and Characterization

Solutions containing equimolar amounts of **A1**–**A4** with dipyridyl donor **D1** in CH_3NO_2/ CH_3OH were stirred for 10 hrs at room temperature, resulting in quantitative self-assembly of **1**–**4**, respectively. Analytically pure metalla-rectangles could be isolated as crystalline solids upon the addition of diethyl-ether to the concentrated reaction mixtures. The ^{1}H NMR spectra for **1**–**4** (Fig. 1)showed characteristic resonances for the pyridyl protons with significant shifts as compared to free **D1**; δ = 8.48 (s, H_4), 8.22 (d, H_1), 8.00 (d, H_3), 7.51 (m, H_2) ppm for **1**; 8.80 (s, H_4), 8.19 (d, $H_{1,3}$), 7.60 (m, H_2) ppm for **2**; 8.85 (s, H_4), 8.56 (d, H_1), 8.07 (d, H_3), 7.53 (m, H_2) ppm for **3**; 9.01 (d, H_4), 8.63 (m, H_1), 7.93 (m, H_3), 7.36 (s, 8H, H_2) ppm for **4**. These resonances were consistent with the assignment of a tetranuclear rectangular structure. The aromatic proton resonances of the *p*-cymene ligands were observed as two doublets around δ = 6.10- 5.7 ppm, while the signals for the benzoquinone protons of **2** (δ = 5.78 ppm) and naphthoquinone protons of **3** (δ = 7.32 ppm) were observed as sharp singlets. The naphthacenedione protons were observed as two multiplets at δ = 8.75 and 7.94 ppm for **4**. The formation of metalla-rectangles **1**–**4** was further confirmed by HR-ESI-MS spectra. The charged states at m/z = 887.9 $[M - 2OTf]^{2+}$ and 542.4 $[M - 3OTf]^{3+}$ for **1**, 937.9 $[M - 2OTf]^{2+}$ and 575.8 $[M - 3OTf]^{3+}$ for **2**, 2125.1 $[M - OTf]^{+}$ for **3**, and 2326.1 $[M - OTf]^{1+}$for **4**, were clearly observed and isotopically resolved. These peaks were all consistent with their theoretical isotopic distributions.

Complexes **5**–**8** self-assembled under identical conditions to those for the formation of **1**–**4**. The proton resonances of the pyridyl groups exhibited similar downfield shifts upon coordination. Signals were observed at 8.38 (m, H_4), 8.17 (m, H_1), 8.12 (m, H_3), 7.52 (m, H_2) ppm for **5**; 8.58 (s, H_4), 8.32(m, H_1), 8.26 (m, H_3), 7.48 (m, H_2) ppm for **6**; 8.72 (s, H_4), 8.63 (m, H_1), 8.12 (m, H_3), 7.59 (m, H_2) ppm for **7**; 8.70 (m, H_4, H_1), 7.75 (m, H_3), 7.33 (m, H_2) ppm for **8.** The *p*-cymene protons were again resolved as two doublets at δ = 6.10- 5.7 ppm. Singlet resonances were observed for the benzoquinone group of **6** (δ = 5.78 ppm) and the naphthoquinone group of **7** (δ = 7.25 ppm). The naphthacenedione protons of **8** were assigned as two multiplets at δ = 8.90 and 8.10 ppm (see Supporting Information†). The ESI mass spectra of **5–8** showed peaks at m/z = 911.9 $[M - 2OTf]^{2+}$ and 558.4 $[M - 3OTf]^{3+}$ for **5**, 2072.4 $[M - OTf]^{+}$ and 592.0 $[M - 3OTf]^{3+}$ for **6,** 625.1 $[M - 3OTf]^{3+}$ for **7** and 1111.8 $[M - 2OTf]^{2+}$ and 692.0 $[M - 3OTf]^{3+}$ for **8**. The peaks were isotopically resolved and agreed well with their corresponding theoretical isotopic distribution patterns (see Supporting Information†).

†Electronic Supplementary Information (ESI) available: [NMR and HR-ESI-MS data for **1–8**, CCDC 841900]. See DOI: 10.1039/b000000x/

NIH-PA Author Manuscript

NIH-PA Author Manuscript

NIH-PA Author Manuscript

Molecular Structure

Single crystals of rectangle **5** were obtained by the slow diffusion of diethyl ether into a methanol/nitromethane solution. Crystals suitable for X-ray diffraction were best grown from the sample of **5** when the counter anion was changed to PF_6^-. A single crystal X-ray diffraction analysis (Table 1) revealed that the complex **5** has a tetranuclear rectangular architecture, which lies on the crystallographic inversion center. Perspective drawings of **5** are shown in Fig. 2 with selected bond lengths and angles listed in Table 2.

Each Ru center adopts a three-legged piano-stool conformation capped by *p*-cymene ligands. The tetradentate dicarboxylate ligands bridge two Ru sites, with the final Ru coordination sites occupied by pyridyl ligands which act as bridges between diruthenium moieties. The pyridine rings are twisted with respect to each other, with an angle of 28.9°. The average Ru–N and Ru–O bond distances are 2.13 and 2.10 Å, respectively. The average bite angle of the two oxygen atoms in the oxalato five-membered chelate rings is 80.9°.

Electronic absorption and fluorescence studies

The UV-Vis spectra of **1**–**8** (Fig. 3) were recorded in methanol solutions resulting in the absorption bands summarized in Table 3. The high energy bands observed in all of the rectangles were also present in the spectra of free **D1** and **D2**. As such, these bands are likely due to **π→π*** transitions of the ethynyl backbone which are preserved upon self-assembly. The dinuclear arene-Ru acceptors also exhibited high-energy absorption bands at 270–298 nm, as well as broad, low-energy absorption bands ranging from 380–680 nm. These bands are likely a combination of intra/intermolecular **π→π*** transitions mixed with metal-to-ligand charge transfers transitions. As with the bands of the pyridyl donors, these arene-Ru-based bands are also preserved upon self-assembly, given rise to complicated absorption manifolds observed for **1**–**8**. [11d]

The emission data for the rectangles and their precursors are summarized in Table 3. The spectrum of **D1** (λ_{ex} = 289 nm) showed a broad band 371 nm. A similar band was observed for **D2**, but tailed significantly further into longer wavelengths, due to its extended **π** system relative to **D1.** This broad peak had features at 360, 387 and 416 nm. Acceptors **A1** and **A2** possessed similar absorption bands centered around 411 nm (Fig. 4, top). The spectra of **A3** and **A4**, however, were markedly different with **A3** displaying a single band around 350 nm and **A4** possessing two bands at 530 and 566 nm (Figure 5). Rectangles **1** and **5** showed emission bands at 381 and 362 nm, respectively (Fig. 4, top). These emission bands likely originate from **D1** and **D2**, which emit in a similar region. Interestingly, rectangle **1** had a similar intensity as to that of the donor with a slight red-shift in position, whereas rectangle **5** showed a quenched intensity compared with **D2**. Rectangles **2** and **6** show emission bands at 335 and 352 nm (**2**) and 335 and 345 nm (**6**) which are blue-shifted slightly from the bands seen for **D1** and **D2**, (Fig. 4, bottom).

For rectangles **3** and **7**, emission bands (λ_{ex} = 330 nm) were observed at 368, 399 and 432 nm (**3**) and 368 and 399 nm (**7**) (Fig. 5, top). Rectangles **4** and **8** showed emission at 527 and 560 nm, respectively, with increased intensity as compared to acceptor **A4** (Fig. 5, bottom). Complexes **3**, **4**, **7** and **8** all share similar emission features with their corresponding arene-Ru precursors, suggesting that the acceptor fragments are the source of emission bands in this subset of rectangles. Metalla-rectangles **1**–**4** qualitatively exhibit stronger bands as compared to **5**–**8**. The more extensive conjugation resulting from the diethynyldipyridyl ligand of the latter may result in enhanced self-quenching and intermolecular **π-π** stacking between two adjacent metalla-rectangles. [16]

NIH-PA Author Manuscript

NIH-PA Author Manuscript

NIH-PA Author Manuscript

In Vitro Anticancer Activity

Organometallic arene-Ru-based half-sandwich complexes have attracted interest as anticancer agents due to their activity against a range of cancer cells with low toxicity and no cross-resistance with cisplatin. The *in vitro* anticancer efficacies of rectangles **1**–**8** and their respective donors were investigated against SK-hep-1(liver cancer) and HCT-15 (colon cancer) human cancer cell lines by means of a colorimetric MTT assay. The results of this assay are summarized in Table 4. Cisplatin and doxorubicin were used as reference compounds. The results demonstrate that **D1**, **D2**, **1** and **2** are inactive (IC_{50} > 200 μM). Complexes **5** and **6** show poor activity, with IC_{50} values between 50–70 μM. Rectangles **3** (IC_{50} = 6.97 and 7.46 μM), **4** (IC_{50} = 29.53 and 39.45 μM), **7** (IC_{50} = 9.60 and 10.66 μM) and **8** (IC_{50} = 16.32 and 17.68 μM) all showed significant activity with IC_{50} values comparable to those determined for cisplatin and doxorubicin. These results suggest that there is no direct correlation between metalla-rectangle size and tumor inhibition efficacy (Fig. 6). The mechanism underlying the anticancer activity of ruthenium compounds is still unclear, but previous findings indicate that the mode of cell cycle regulation by Ru complexes is different from that of cisplatin. During apoptosis, cisplatin blocks cancer cell growth in the G2-phase[17] whereas the arene-Ru-based metalla-cycles arrest cell growth in the G1 phase.[13a] The different modes of action during cell cycle progression of cisplatin and arene-Ru-based metalla-cycles suggest that these two classes of complexes have different mechanisms of action.[18]

Conclusion

We have synthesized eight new tetranuclear rectangles of varying size by coordination driven self-assembly between arene-Ru-based acceptors and 3-dipyridyl donors. All of these molecules were well-characterized by multinuclear NMR (^{1}H and ^{13}C) and HR-ESI-MS data. The solid state structure of **5** was confirmed by single crystal diffraction studies. UV-Vis and fluorescence studies were also carried out, indicating that the photophysical properties of the assemblies largely mimicked those of their precursors. The cytotoxicity of these metalla-rectangles against SK-hep-1 and HCT-15 human cancer cell lines was evaluated with complexes **3**, **4**, **7** and **8** exhibiting low IC_{50} values on the order of cisplatin and doxorubicin.

Supplementary Material

Refer to Web version on PubMed Central for supplementary material.

Acknowledgments

This work was supported by the World Class University (WCU) program (R33-2008-000-10003) and Priority Research Centers program (2009-0093818) through the National Research Foundation of Korea (NRF) funded by the Ministry of Education, Science and Technology. X-ray diffraction experiments using synchrotron radiation were performed at the Pohang Accelerator Laboratory in Korea. P.J.S thanks the NIH (GM-57052) for financial support.

References

1. (a) Leininger S, Olenyuk B, Stang PJ. Chem. Rev. 2000; 100:853–907. [PubMed: 11749254] (b) Stang PJ, Olenyuk B. Acc. Chem. Res. 1997; 30:502–518.(c) Fujita M. Chem. Soc. Rev. 1998; 27:417–425.(d) Holliday BJ, Mirkin CA. Angew. Chem., Int. Ed. 2001; 40:2022–2043.(e) Cotton FA, Lin C, Murillo CA. Acc. Chem. Res. 2001; 34:759–771. [PubMed: 11601960] (f) Sun S–S, Stern CL, Nguyen ST, Hupp JT. J. Am. Chem. Soc. 2004; 126:6314–6326. [PubMed: 15149229] (g) Gianneschi NC, Masar MS III, Mirkin CN. Acc. Chem. Res. 2005; 38:825–837. [PubMed: 16285706] (h) Qin Z, Jennings MC, Puddephatt RJ. Inorg. Chem. 2002; 41:3967–3974. [PubMed:

NIH-PA Author Manuscript

NIH-PA Author Manuscript

NIH-PA Author Manuscript

12132923] (i) Habermehl NC, Jennings MC, McArdle CP, Mohr F, Puddephatt RJ. Organometallics. 2005; 24:5004–5014.(j) Badjic JD, Nelson A, Cantrill SJ, Turnbull WB, Stoddart JF. Acc. Chem. Res. 2005; 38:723–732. [PubMed: 16171315] (k) Nehete UN, Chandrasekhar V, Anantharaman G, Roesky HW, Vidovic D, Magul J. Angew. Chem., Int. Ed. 2004; 43:3842–3844. (l) Chai J, Jancik V, Singh S, Zhu H, He C, Roesky HW, Schmidt H–G, Noltemeyer M, Hosmane NS. J. Am. Chem. Soc. 2005; 127:7521–7528. [PubMed: 15898803]

2. (a) Stulz E, Ng Y–F, Scott SM, Sanders JKM. Chem. Commun. 2002:524–525.(b) Schmittel M, Mahata K. Angew. Chem., Int. Ed. 2008; 47:5284–5286.(c) Schmittel M, Kalsani V, Kishore RSK, Co¨lfen H, Bats JW. J. Am. Chem. Soc. 2005; 127:11544–11545. [PubMed: 16104698] (d) Schmittel M, Mahata K. Inorg. Chem. 2009; 48:822–824. [PubMed: 19128046] (e) Yang H–B, Ghosh K, Northrop BH, Zheng Y–R, Lyndon MM, Muddiman DC, Stang PJ. J. Am. Chem. Soc. 2007; 129:14187–14189. [PubMed: 17963382]
3. (a) Ghosh K, Yang H–B, Northrop BH, Lyndon MM, Zheng Y–R, Muddiman DC, Stang PJ. J. Am. Chem. Soc. 2008; 130:5320–5334. [PubMed: 18341280] (b) Baxter P, Lehn J–M, DeCian A, Fischer J. Angew. Chem., Int. Ed. 1993; 32:69–72.(c) Chichak KS, Cantrill SJ, Pease AR, Chiu S–H, Cave GWV, Atwood JL, Stoddart JF. Science. 2004; 304:1308–1312. [PubMed: 15166376] (d) Cho YL, Uh HS, Chang S–Y, Chang H–Y, Choi M–G, Shin I, Jeong K–S. J. Am. Chem. Soc. 2001; 123:1258–1259. [PubMed: 11456692] (e) Lee J, Ghosh K, Stang PJ. J. Am. Chem. Soc. 2009; 131:12028–12029. [PubMed: 19663439] (f) Mahata K, Schmittel M. J. Am. Chem. Soc. 2009; 131:16544–16554. [PubMed: 19860466]
4. (a) Kishore RSK, Paululat T, Schmittel M. Chem. Eur. J. 2006; 12:8136–8149. [PubMed: 16862633] (b) Yamauchi Y, Fujita M. Chem. Commun. 2010; 46:5897–5899.(c) Yamanaka M, Yamada Y, Sei Y, Yamaguchi K, Kobayashi K. J. Am. Chem. Soc. 2006; 128:1531–1539. [PubMed: 16448123] (d) Kumazawa K, Biradha K, Kusukawa T, Okano T, Fujita M. Angew. Chem., Int. Ed. 2003; 42:3909–3913.(e) Yoshizawa M, Nakagawa J, Kurnazawa K, Nagao M, Kawano M, Ozeki T, Fujita M. Angew. Chem., Int. Ed. 2005; 44:1810–1813.(f) Wang M, Lan WJ, Zheng Y-R, Cook TR, White HS, Stang Peter J. J. Am. Chem. Soc. 2011; 133:10752–10755. [PubMed: 21671637] (g) Blanco V, Garc´a MD, Platas-Iglesias C, Peinador C, Quintela JM. Chem. Commun. 2010:6672–6674.
5. (a) Northrop BH, Yang H–B, Stang PJ. Chem. Commun. 2008:5896–5908.(b) Parkash MJ, Lah MS. Chem. Commun. 2009:3326–3341.(c) Zheng YR, Zhao Z, Kim H, Wang M, Ghosh K, Pollock JB, Chi K–W, Stang PJ. Inorg. Chem. 2010; 49:10238–10240. [PubMed: 20949905] (d) Hof F, Craig SL, Nuckolls C, Rebek J Jr. Angew. Chem. 2002; 114:1556–1578.Angew. Chem. Int. Ed. 2002; 41:1488–1508.
6. (a) Rebek J Jr. Angew. Chem. 2005; 117:2104–2115.Angew. Chem. Int. Ed. 2005; 44:2068–2078. (b) Vriezema DM, Aragones MC, Elemans JAAW, Cornelissen JJLM, Rowan AE, Nolte RJM. Chem. Rev. 2005; 105:1445–1489. [PubMed: 15826017] (c) Yoshizawa M, Klosterman JK, Fujita M. Angew. Chem. Int. Ed. 2009; 48:3418–3438.(d) Nishioka Y, Yamaguchi T, Yoshizawa M, Fujita M. J. Am. Chem. Soc. 2007; 129:7000–7001. [PubMed: 17497783] (e) Inokuma Y, Arai T, Fujita M. Nature Chem. 2010; 2:780–783. [PubMed: 20729900] (f) Inokuma Y, Yoshioka S, Fujita M. Angew. Chem. Int. Ed. 2010; 49:8912–8914.
7. (a) Kuehl CJ, Huang SD, Stang PJ. J. Am. Chem. Soc. 2001; 123:9634–9641. [PubMed: 11572685] (b) Moriuchi T, Miyaishi M, Hirai T. Angew. Chem. Int. Ed. 2001; 40:3042–3045.(c) Caskey DC, Shoemaker RK, Michl J. Org. Lett. 2004; 6:2093–2096. [PubMed: 15200293] (d) Kim D, Paek JH, Jun M-J, Lee JY, Kang SO, Ko J. Inorg. Chem. 2005; 44:7886–7894. [PubMed: 16241138] (e) Seidel SR, Stang PJ. Acc. Chem. Res. 2002; 35:972–983. [PubMed: 12437322] (f) Vajpayee V, Kim H, Mishra A, Mukherjee PS, Stang PJ, Lee MH, Kim HK, Chi K-W. Dalton Trans. 2011; 40:3112–3115. [PubMed: 21321785]
8. (a) Fujita M, Tominaga M, Hori A, Therrien B. Acc. Chem. Res. 2005; 38:369–378. [PubMed: 15835883] (b) Oliver CG, Ulman PA, Wiester MJ, Mirkin CA. Acc. Chem. Res. 2008; 41:1618–1629. [PubMed: 18642933] (c) Chakrabarty R, Mukherjee PS, Stang PJ. Chem. Rev. 2011(d) Resendiz MJE, Noveron JC, Disteldorf H, Fischer S, Stang PJ. Org. Lett. 2004; 6:651–653. [PubMed: 14986941] (e) Kuehl C, Huang SD, Stang PJ. J. Am. Chem. Soc. 2001; 123:9634–9641. [PubMed: 11572685] (f) Kuehl C, Mayne CL, Arif AM, Stang PJ. Org. Lett. 2000; 2:3727–3729. [PubMed: 11073686] (g) Kaim W, Schwederski B, Dogan A, Fiedler J, Kuehl CJ, Stang PJ. Inorg. Chem. 2002; 41:4025–4028. [PubMed: 12132929]

NIH-PA Author Manuscript

NIH-PA Author Manuscript

NIH-PA Author Manuscript

9. (a) Dinolfo PH, Williams ME, Stern CL, Hupp JT. J. Am. Chem. Soc. 2004; 126:12989–13001. [PubMed: 15469297] (b) Benkstein KD, Hupp JT, Stern CL. Angew. Chem., Int. Ed. 2000; 39:2891–2893.(c) Dinolfo PH, Hupp JT. Chem. Mater. 2001; 13:3113–3125.(d) Liao R-T, Yang W-C, T P, Tsai C-C, S M, Liu Y-H, Rajendran T, Lin H-M, Tseng T-W, Lu K-L. Chem. Commun. 2008:3175–3177.
10. (a) Han Y-F, Jia W-G, Yu W-B, Jin G-X. Chem. Soc. Rev. 2009:3419–3434. [PubMed: 20449060] (b) Boyer JL, Kuhlman ML, Rauchfuss TB. Acc. Chem. Res. 2007; 40:233–242. [PubMed: 17284016] (c) Severin K. Chem. Commun. 2006:3859–3867.(d) Han Y–F, Li H, Jin G-X. Chem. Commun. 2010; 46:6879–6890.(e) Han Y-F, Lin Y-J, Weng L-H, Berke H, Jin G-X. Chem. Commun. 2008:350–352.
11. (a) Yan H, Süss-Fink G, Neels A, Stoeckli-Evans H. J. Chem. Soc., Dalton Trans. 1997:4345–4350.(b) Zhang W-Z, Han Y-F, Lin Y-J, Jin G-X. Dalton Trans. 2009:8426–8431. [PubMed: 19789798] (c) Han Y-F, Fei Y, Jin G-X. Dalton Trans. 2010; 39:3976–3984. [PubMed: 20372723] (d) Vajpayee V, Song YH, Lee MH, Kim H, Wang M, Stang PJ, Chi K–W. Chem. Eur. J. 2011; 17:7837–7844. [PubMed: 21611989] (e) Wang M, Vajpayee V, Shanmugaraju S, Zheng YR, Zhao Z, Kim H, Mukherjee PS, Chi K–W, Stang PJ. Inorg. Chem. 2011; 50:1506–1512. [PubMed: 21214171]
12. (a) Therrien B. Eur. J. Inorg. Chem. 2009:2445–2453.(b) Barry NPE, Furrer J, Freudenreich J, Süss-Fink G, Therrien B. Eur. J. Inorg. Chem. 2010:725–728.(c) Vieille-Petit L, Therrien B, Süss-Fink G, Ward TR. J. Organomet. Chem. 2003; 684:117–123.(d) Ang WH, Grote Z, Scopelliti R, Juillerat-Jeanneret L, Severin K, Dyson PJ. J. Organomet. Chem. 2009; 694:968–972.(e) Govender P, Renfrew AK, Clavel CM, Dyson PJ, Therrien B, Smith GS. Dalton Trans. 2011; 40:1158–1167. [PubMed: 21165516]
13. (a) Vajpayee V, Yang YJ, Kang SC, Kim H, Kim IS, Wang M, Stang PJ, Chi K-W. Chem. Commun. 2011; 47:5184–5186.(b) Barry NPE, Edafe F, Therrien B. Dalton Trans. 2011; 40:7172–7180. [PubMed: 21660364] (c) Linares F, Galindo MA, Galli S, Romero MA, Navarro JAR, Barea E. Inorg. Chem. 2009; 48:7413–7420. [PubMed: 19586019] (d) Barry NPE, Zava O, Furrer J, Dyson PJ, Therrien B. Dalton Trans. 2010; 39:5272–5277. [PubMed: 20442944] (e) Therrien B, Süss-Fink G, Govindaswamy P, Renfrew AK, Dyson PJ. Angew. Chem., Int. Ed. 2008; 47:3773–3776.(f) Zava O, Mattsson J, Therrien B, Dyson PJ. Chem.–Eur. J. 2010; 16:1428–1431. [PubMed: 20033971] (g) Pitto-Barry A, Barry NPE, Zava O, Deschenaux R, Therrien B. Chem. – Asian J. 2011; 6:1595–1603. [PubMed: 21626704] (h) Barry NPE, Abd Karim NH, Vilar R, Therrien B. Dalton Trans. 2009:10717–10719. [PubMed: 20023899] (i) Smith GS, Therrien B. Dalton Trans. 2011
14. (a) Vajpayee V, Song YH, Yang YJ, Kang S, Kim H, Kim IS, Wang M, Stang PJ, Chi K–W. Organometallics. 2011; 30:3242–3245. [PubMed: 21779140] (b) Mattsson J, Govindaswamy P, Renfrew AK, Dyson PJ, Štěpnička P, Süss-Fink G, Therrien B. Organometallics. 2009; 28:4350–4357.(c) Linares F, Procopio EQ, Galindo MA, Romero MA, Navarro JAR, Barea E. CrystEngComm. 2010; 12:2343–2346.
15. Chi K-W, Addicott C, Arif AM, Das N, Stang PJ. J. Org. Chem. 2003; 68:9798–9801. [PubMed: 14656109]
16. Shanmugam S, Bar AK, Joshi S, Patil YP, Mukherjee PS. Organometallics. 2011; 30:1951–1960.
17. Siddik ZH. Oncogene. 2003; 22:7265–7279. [PubMed: 14576837]
18. Kisova A, Zerzankova L, Habtemariam A, Sadler PJ, Brabec V, Kasparkova J. Mol. Pharmaceutics. 2011; 8:949–957.

NIH-PA Author Manuscript
NIH-PA Author Manuscript
NIH-PA Author Manuscript

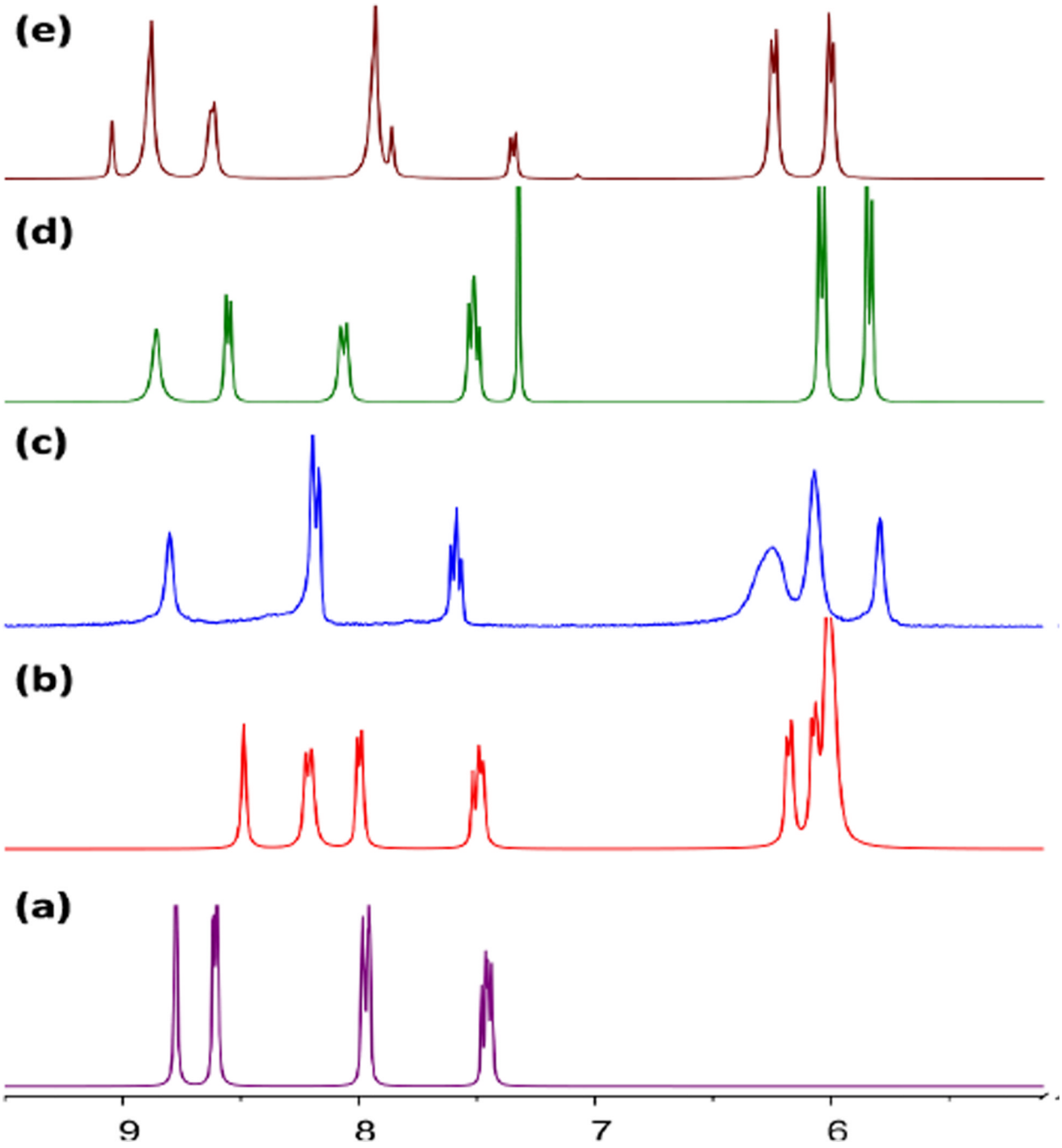

Fig. 1.
Partial ^{1}H NMR spectra of the metalla-rectangles **1**(b), **2**(c), **3**(d), **4**(e) and donor **D1**(a).

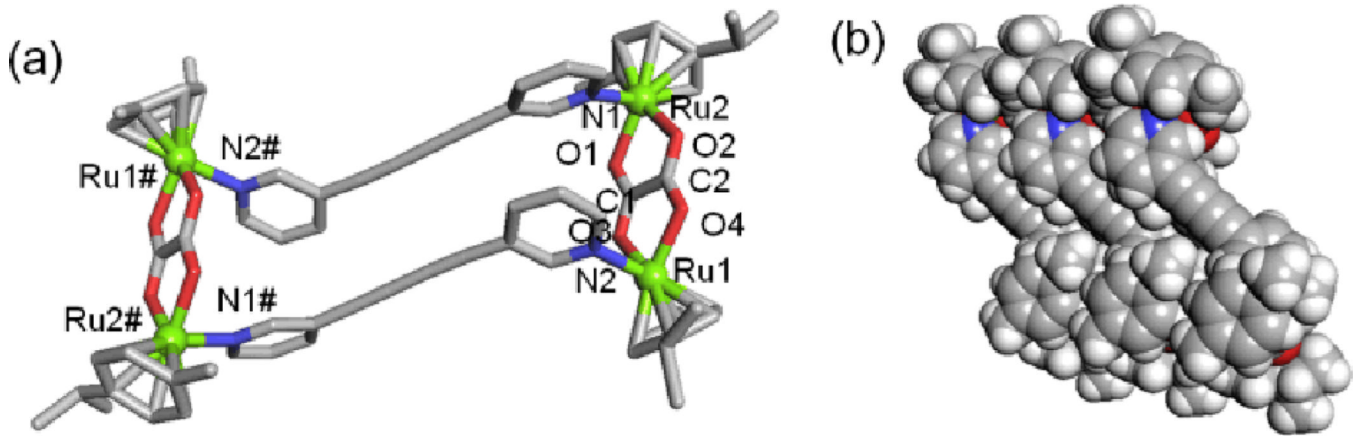

Fig. 2.

(a) X-ray crystal structure of metalla-rectangle **5**. Solvent molecules, counter-anions and hydrogen atoms are omitted for clarity (Color codes: green = Ru, red = O, blue = N and grey = C). (b) Crystal packing diagram of **5** with a space-filling model. The mark (#) on atom labels denote the elements generated by inversion symmetry (−x, −y, −z).

NIH-PA Author Manuscript NIH-PA Author Manuscript NIH-PA Author Manuscript

NIH-PA Author Manuscript

NIH-PA Author Manuscript

NIH-PA Author Manuscript

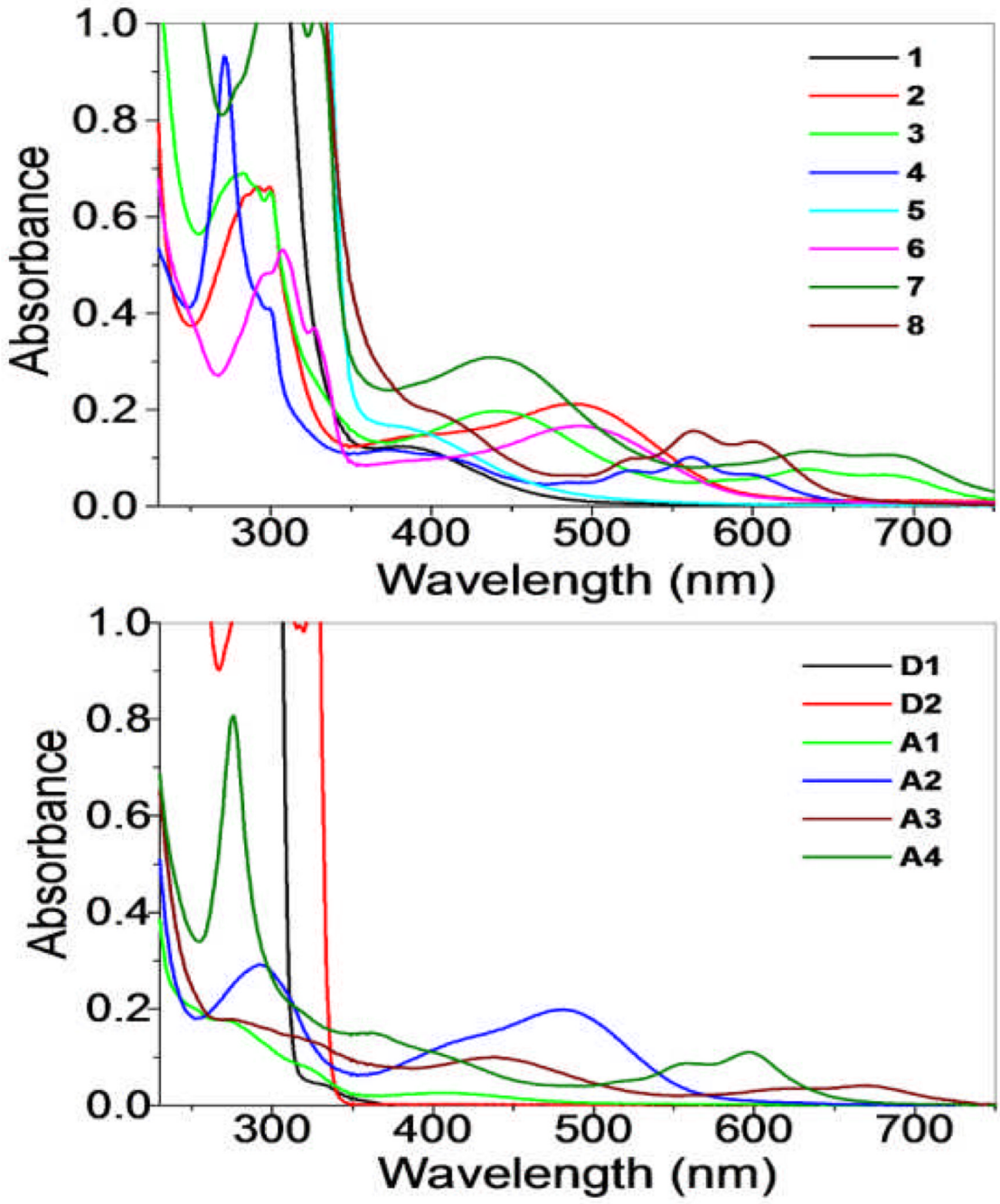

Fig. 3.
UV-Vis spectra of metalla-rectangles **1**–**8** (left) and their donor (**D1**, **D2**) and acceptors (**A1**–**A4**)(right).

NIH-PA Author Manuscript
NIH-PA Author Manuscript
NIH-PA Author Manuscript

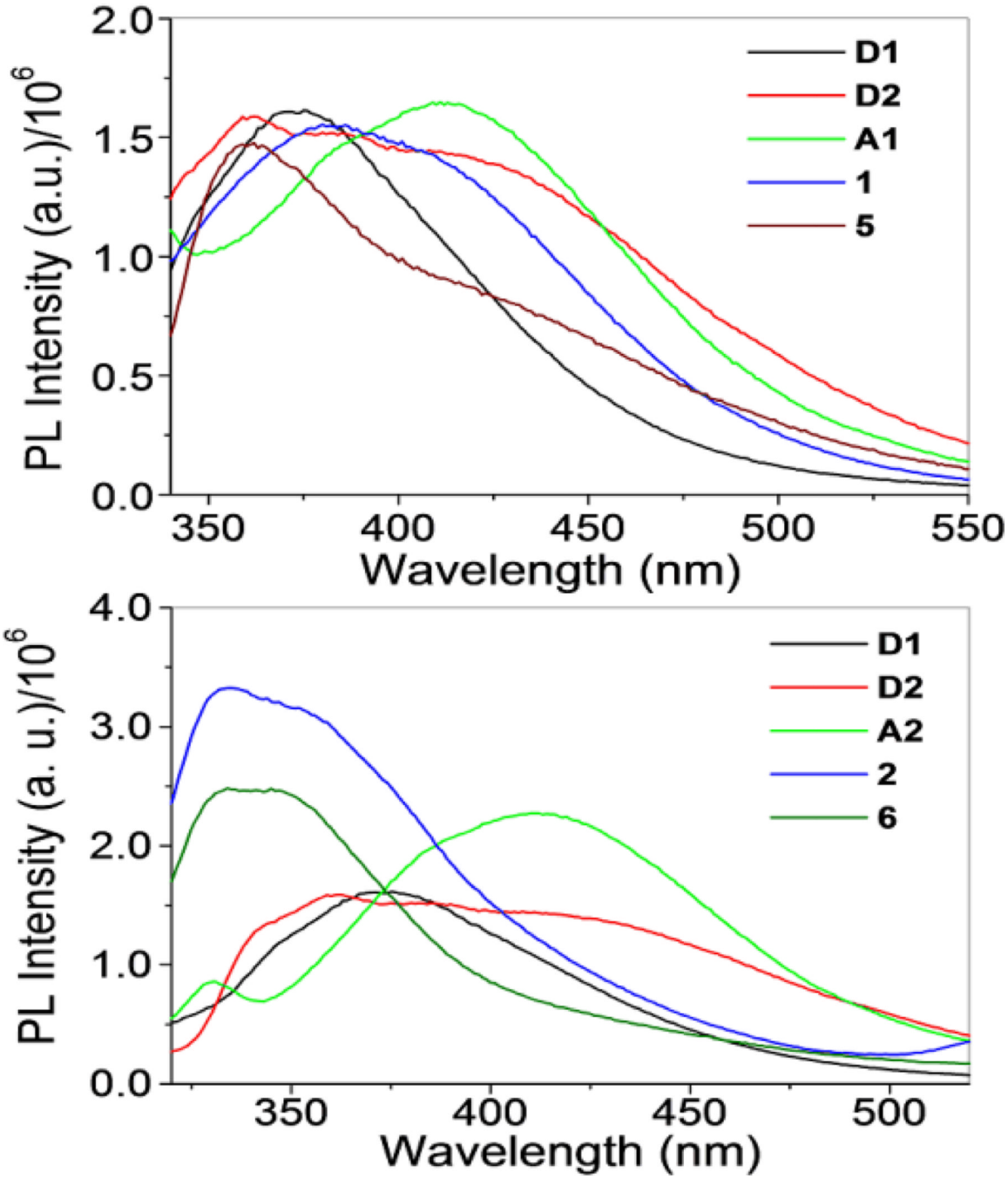

Fig. 4.
Emission spectra of metalla-rectangles **1** and **5** (top) and **2** and **6**(bottom) compared with their respective donors and acceptors.

NIH-PA Author Manuscript
NIH-PA Author Manuscript
NIH-PA Author Manuscript

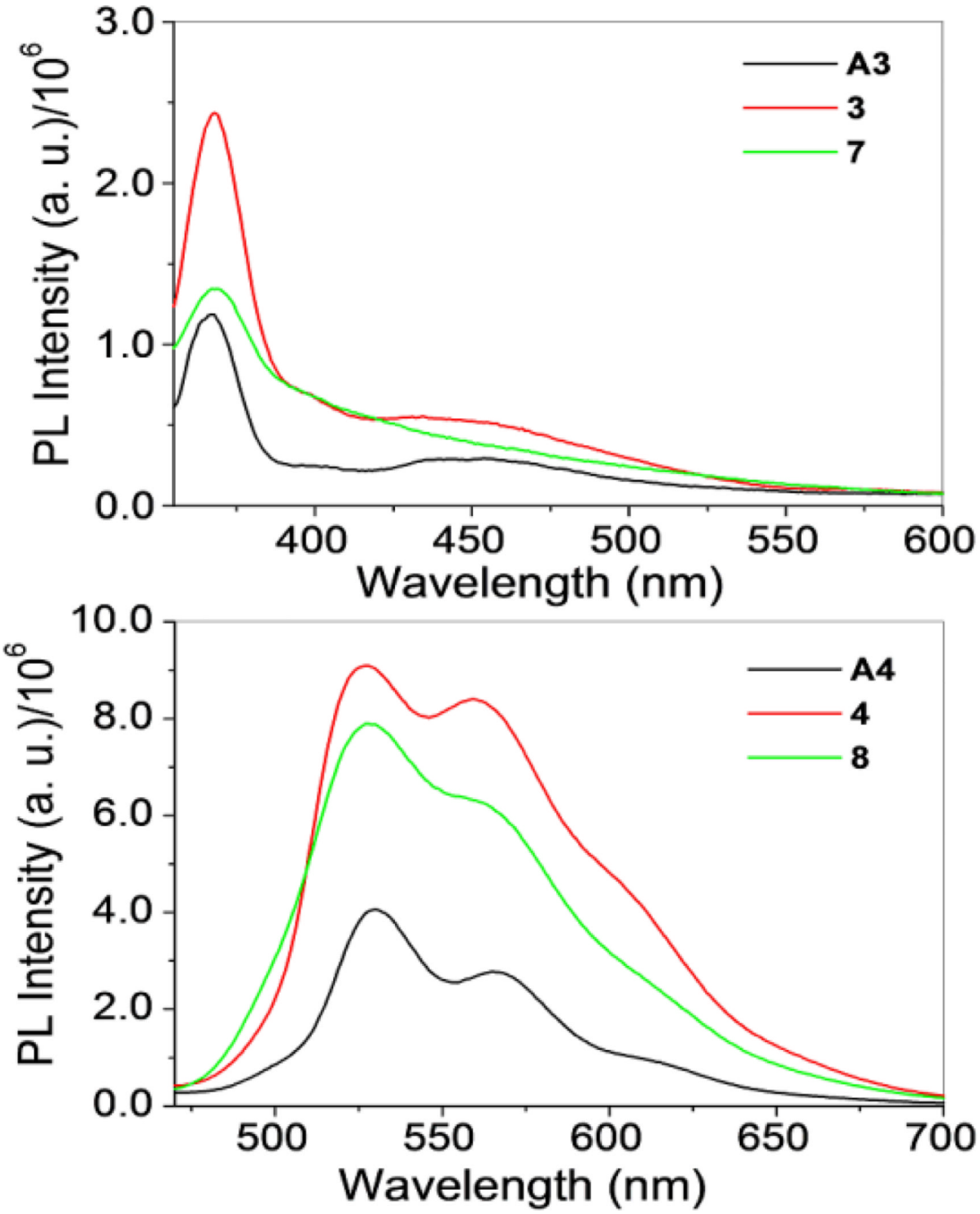

Fig. 5.
Emission spectra of metalla-rectangles **3** and **7** (top) and **4** and **8**(bottom) compared with their acceptors.

NIH-PA Author Manuscript
NIH-PA Author Manuscript
NIH-PA Author Manuscript

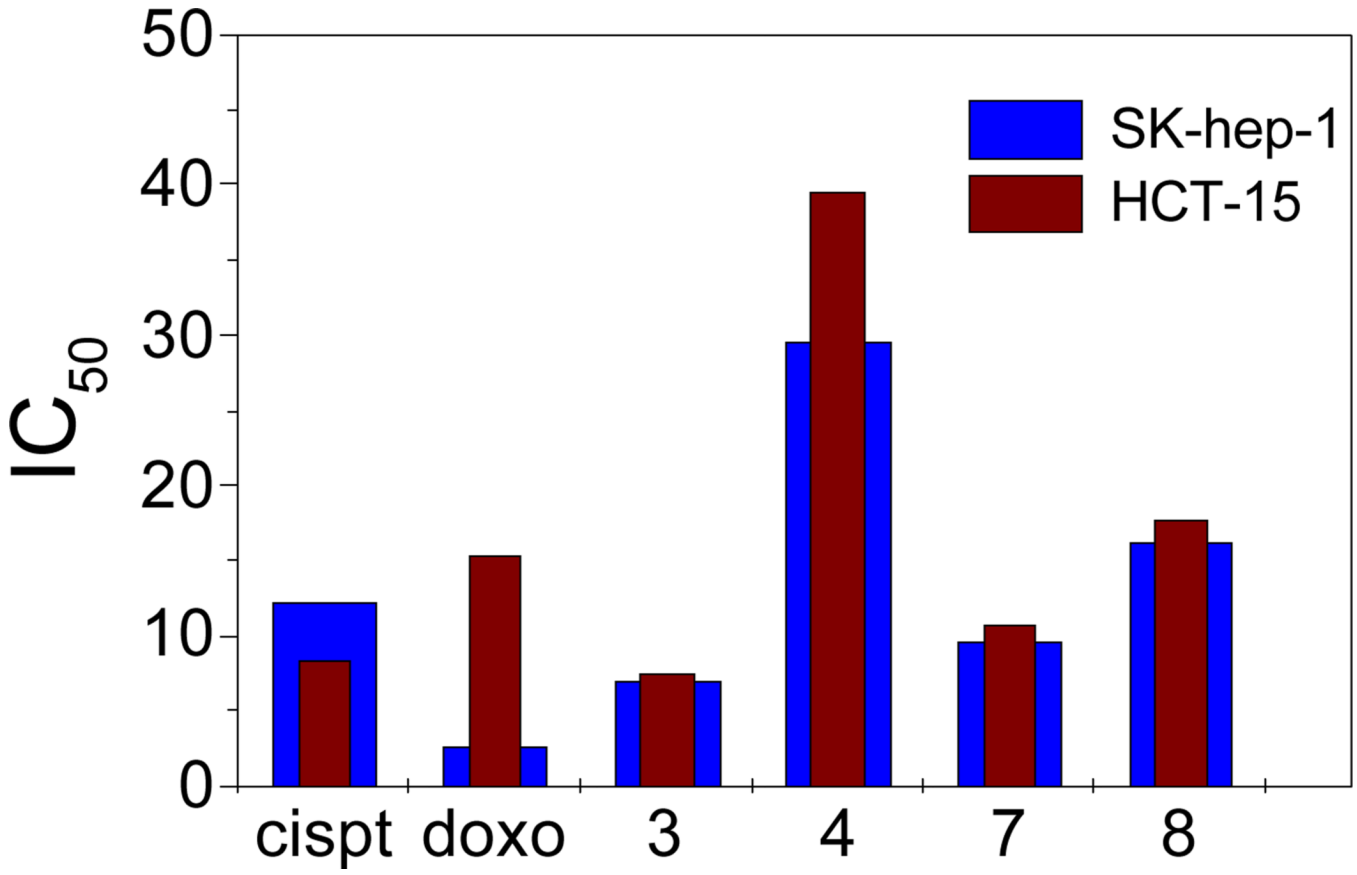

Fig 6.
Comparison of cytotoxicities of **3**, **4**, **7** and **8** with cisplatin and doxorubicin.

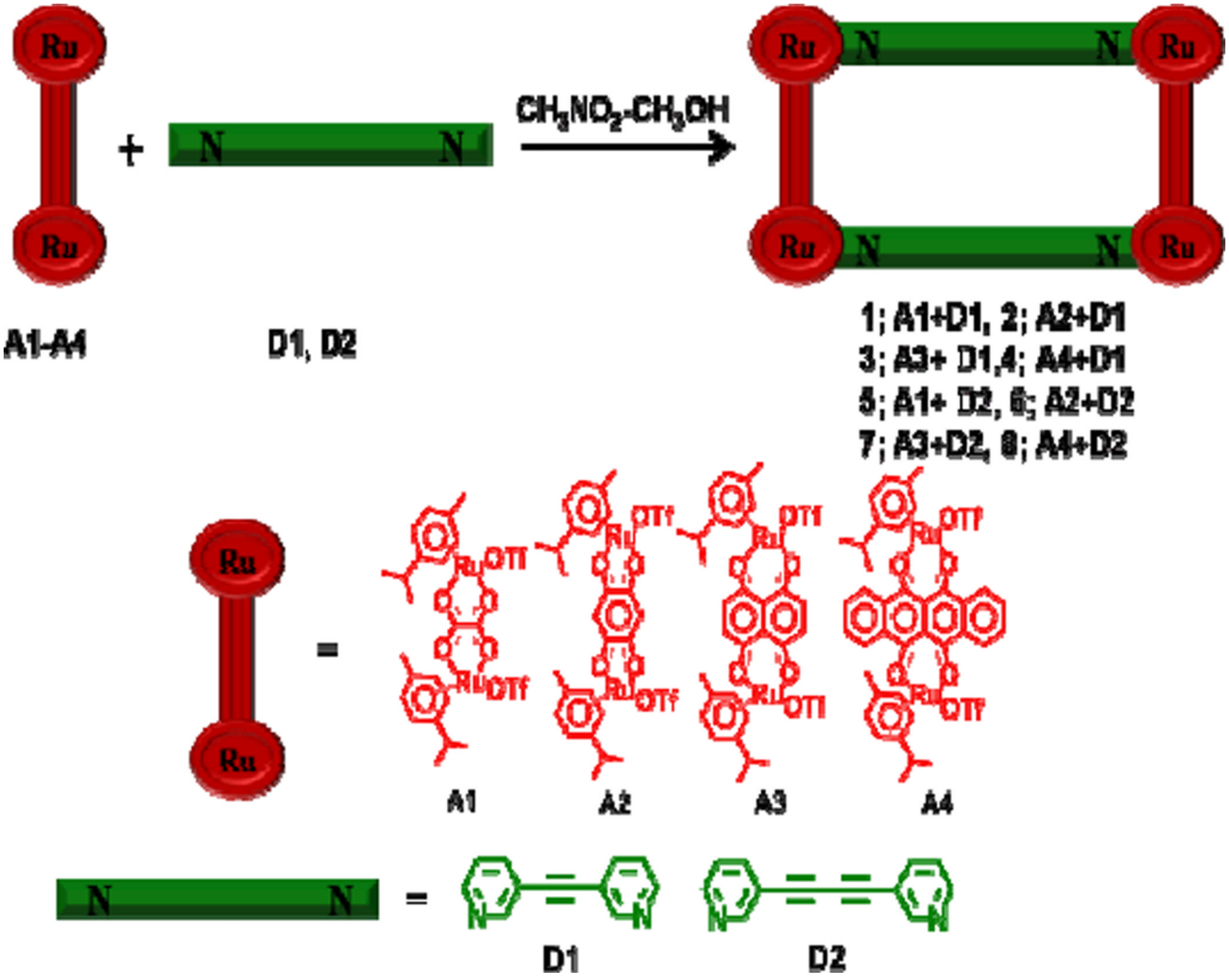

Scheme 1.
Coordination-driven self-assembly of molecular-rectangles **1**–**8**.

NIH-PA Author Manuscript
NIH-PA Author Manuscript
NIH-PA Author Manuscript

NIH-PA Author Manuscript

NIH-PA Author Manuscript

NIH-PA Author Manuscript

Table 1

Crystal data and structure refinement for molecular rectangle **5**.

Empirical formula	$C_{36.50}\ H_{37.50}\ F_{12}\ N_{2.50}\ O_5\ P_2\ Ru_2$
Formula weight	1083.27
Temperature	100(2) K
Wavelength	0.90000 Å
Crystal system	Monoclinic
Space group	$P2_1/n$
Unit cell dimensions	a = 8.630(2) Å α = 90° b = 35.969(7) Å β = 97.55(3)° c = 13.430(3) Å γ = 90°
Volume	4132.7(14) $Å^3$
Z	4
$D_{calculated}$	1.741 g/cm^3
Abs. coefficient	1.697 mm^{-1}
Goodness-of-fit on F^2	1.023
Final R indices [I>2sigma(I)]	R1 = 0.0550, wR2 = 0.1557
R indices (all data)	R1 = 0.0679, wR2 = 0. 1656
Largest diff. peak and hole	1.040 and −1.025 e.$Å^{-3}$

NIH-PA Author Manuscript

NIH-PA Author Manuscript

NIH-PA Author Manuscript

Table 2

Bond lengths [Å] and angles [°] for **5**.

Ru(1)-O(4)	2.105(5)	Ru(1)-O(3)	2.104(5)
Ru(1)-N(2)#1	2.127(6)	Ru(1)-C(27)	2.174(8)
Ru(2)-O(1)	2.112(5)	Ru(2)-N(1)	2.109(6)
Ru(2)-O(2)	2.110(6)		
O(4)-Ru(1)-O(3)	78.8(2)	O(4)-Ru(1)-N(2)#1	84.4(2)
O(3)-Ru(1)-N(2)#1	81.7(2)	O(4)-Ru(1)-C(30)	93.9(3)
N(2)#1-Ru(1)-C(30)	125.6(3)	N(2)#1-R u(1)-C (27)	115.3(3)
O(1)-Ru(2)-N(1)	84.5(2)	N(1)-Ru(2)-O(2)	82.6(2)
O(1)-Ru(2)-C(3)	90.4(2)		

NIH-PA Author Manuscript

NIH-PA Author Manuscript

NIH-PA Author Manuscript

Table 3

Photophysical Properties of the metalla-rectangles **1–8**.

Molecular-rectangle	Absorption maxima λ_{max}(nm) (Molar extinction co-efficient 10^5 ε M^{-1} cm^{-1})	λ_{ex}(nm)	Emission maxima λ_{max}(nm)
1	280 (2.54), 382(0.12)	298	362, 381
2	292 (0.66), 491 (0.30)	298	335, 352
3	280 (1.02), 437 (0.29), 633 (0.11), 690 (0.09)	330	368, 432
4	272 (1.39), 377(0.17), 562 (0.15), 598 (0.10)	390	527, 560
5	296(2.04), 307(2.23), 327 (1.59), 376 (0.16)	298	362, 381
6	297(0.58), 307(0.64), 327 (0.44), 491 (0.20)	298	335, 345
7	297(1.05), 311(1.24), 328 (1.02), 437 (0.31), 633(0.11), 694 (0.10)	330	368
8	272 (2.52), 377(1.20), 562 (0.15), 602 (0.13)	390	527, 560

NIH-PA Author Manuscript

NIH-PA Author Manuscript

NIH-PA Author Manuscript

Table 4

IC_{50} values for SK-hep-1 and HCT-15 human cancer cells for molecular rectangles **1–8**, donors, cisplatin and dxorubicin.

compound	IC_{50} μM[a]	
	SK-hep-1	**HCT-15**
1	>200	>200
2	>200	>200
3	6.97±0.69	7.46±0.24
4	29.53±1.72	39.45±1.73
5	66.19±0.25	53.66±0.27
6	63.58±1.27	57.05±0.98
7	9.60±0.84	10.66±0.19
8	16.32±1.98	17.68±0.92
D1	>200	>200
D2	>200	>200
cisplatin	12.38±0.24	8.38±2.31
doxorubicin	2.67±0.24	15.34±0.58

[a] IC_{50}: drug concentration necessary for 50% inhibition of cell viability.